# PACAP modulation of the colon–inferior mesenteric ganglion reflex in the guinea pig

Leonid G. Ermilov[1,2], Philip F. Schmalz[1,2], Steven M. Miller[1,2] and Joseph H. Szurszewski[1,2,3]

[1]*Department of Physiology and Biomedical Engineering,* [2]*Enteric NeuroScience Program and* [3]*Division of Gastroenterology and Hepatology, Mayo Clinic College of Medicine, 200 First Street, SW, Rochester, MN 55905 USA*

**We investigated the effect of pituitary adenylate cyclase activating peptide (PACAP) on the colon–inferior mesenteric ganglion (IMG) reflex loop *in vitro*. PACAP27 and PACAP38 applied to the IMG caused a prolonged depolarization and intense generation of fast EPSPs and action potentials in IMG neurones. Activation of PACAP-preferring receptors (PAC1-Rs) with the selective agonist maxadilan or vasoactive intestinal peptide (VIP)/ PACAP (VPAC) receptors with VIP produced similar effects whereas prior incubation of the IMG with selective PAC1-R antagonists PACAP6-38 and M65 inhibited the effects of PACAP. Colonic distension evoked a slow EPSP in IMG neurones that was reduced in amplitude by prolonged superfusion of the IMG with either PACAP27, maxidilan, PACAP6-38, M65 or VIP. Activation of IMG neurones by PACAP27 or maxadilan resulted in an inhibition of ongoing spontaneous colonic contractions. PACAP-LI was detected in nerve trunks attached to the IMG and in varicosities surrounding IMG neurones. Cell bodies with PACAP-LI were present in lumbar 2–3 dorsal root ganglia and in colonic myenteric ganglia. Colonic distension evoked release of PACAP peptides in the IMG as measured by radioimmunoassay. Volume reconstructed images showed that a majority of PACAP-LI, VIP-LI and VAChT-LI nerve endings making putative synaptic contact onto IMG neurones and a majority of putative receptor sites containing PAC1-R-LI and nAChR-LI on the neurones were distributed along secondary and tertiary dendrites. These results suggest involvement of a PACAP-ergic pathway, operated through PAC1-Rs, in controlling the colon–IMG reflex.**

(Received 15 June 2004; accepted after revision 27 July 2004; first published online 29 July 2004)
**Corresponding author** J. H. Szurszewski: Department of Physiology and Biomedical Engineering, Mayo Clinic College of Medicine, 200 First Street SW, Rochester, MN 55905, USA. Email: gijoe@mayo.edu

Intestinofugal afferent neurones (IFANs) are a subset of myenteric ganglion neurones that relay mechanosensory information to sympathetic neurones in the abdominal prevertebral ganglia (Furness *et al.* 1999; Szurszewski *et al.* 2002; Ermilov *et al.* 2003). They function physiologically as slowly adapting mechanoreceptors that detect changes in intraluminal volume of the intestine (Weems & Szurszewski, 1978; Szurszewski & Miller, 1994; Miller & Szurszewski, 2002). The IFANs are functionally arranged in parallel to the circular muscle fibres (Szurszewski & Miller, 1994; Szurszewski *et al.* 2002) and they respond to stretch of the circular muscle rather than to tension (Miller & Szurszewski, 2003). When activated by distension, IFANs release acetylcholine in the prevertebral ganglia to evoke nicotinic fast excitatory postsynaptic potentials (F-EPSPs) (Crowcroft *et al.* 1971; Parkman *et al.* 1993; Szurszewski *et al.* 2002) and VIP to evoke a slow excitatory postsynaptic potential (S-EPSP) which increases the efficiency of cholinergic nicotinic synaptic transmission. Prevertebral ganglion neurones that receive synaptic input from IFANs project their axons back to the same or different regions of the gastrointestinal tract where they modulate motility and possibly also secretion (Szurszewski & Miller, 1994).

In a preliminary study (Ermilov & Szurszewski, 1998), we found that PACAP, a member of the secretin/glucagon/VIP family of regulatory peptides, increased the excitability of sympathetic neurones of the inferior mesenteric ganglion (IMG) of the guinea pig, raising the possibility that PACAP is an important neuromodulator of sympathetic nerves that regulate gut motility. To date, there have been no comprehensive studies on whether PACAP peptides alter synaptic transmission in prevertebral ganglia, nor is there any information on the nature of the receptor that mediates the actions of PACAP peptides on prevertebral ganglion neurones. The absence of this information was one of the reasons for doing this study. Another objective

 DOI: 10.1113/jphysiol.2004.070060

of our study was to map the spatial distribution of presumptive PACAP-containing presynaptic structures as well as the spatial distribution of PACAP-preferring receptors (PAC1-Rs) on IMG neurones. Recently, we described techniques that combine intracellular injection of single neurones in whole mount preparations with confocal laser scanning microscopy and three dimensional (3-D) reconstruction to reveal the 3-D structure of single myenteric ganglion neurones and the distribution of nicotinic acetylcholine receptors (nAChRs) on IFANs (Ermilov *et al.* 2000; Ermilov *et al.* 2003). We applied these methods in the present study to assess the spatial distribution of putative synaptic regions immunopositive for PACAP, VIP and acetylcholine on single IMG neurones and to provide quantitative data on the spatial distribution of PAC1-Rs and nAChRs. Parts of this study were communicated previously in abstract form (Ermilov *et al.* 2001).

## Methods

### General procedures

Dunkin-Hartley male guinea pigs weighing 250–300 g were killed by $CO_2$ asphyxiation as approved by the Animal Care and Use Committee of the Mayo Clinic and Foundation. The IMG, dorsal root ganglia (DRG) $L_2$ and $L_3$, and segments of distal colon were used in different experiments.

### Intracellular recording

The IMG alone or attached via lumbar colonic nerves to a 3–4 cm segment of distal colon was rapidly dissected and placed into a two-compartment organ bath as previously described (Ermilov & Kaliunov, 1983; Parkman *et al.* 1993). Both compartments were separately perfused at 3 ml $min^{-1}$ with normal Krebs solution (NKS) of the following composition (mM): $Na^+$ 137.4, $K^+$ 5.9, $Ca^{2+}$ 2.5, $Mg^{2+}$ 1.2, $Cl^-$ 134, $HCO_3^-$ 15.5, $H_2PO_4^-$ 1.2 and glucose 11.5, bubbled with 97% $O_2$ and 3% $CO_2$. Colonic intraluminal pressure was monitored with a pressure transducer (Chex-All II, recorder no. 024010, Propper Inc., Long Island City, NY, USA) as previously described (Miller *et al.* 1997).

Intracellular recordings were obtained from ganglion neurones by conventional sharp microelectrode techniques using borosilicate glass micropipettes filled with 3 M KCl (tip resistance 60–100 MΩ) connected to a high impedance amplifier (Duo 773; WPI Inc., Sarasota, FL, USA) containing an active bridge circuit. Electrical signals were displayed on a dual beam oscilloscope (R 5103N; Tektronix, Inc., Beaverton, OR, USA), recorded on a chart recorder (Gould Inc., Cleveland, OH, USA) and stored on FM tape (recorder model 3964A; Hewlett Packard, Loveland, CA, USA) for subsequent analysis with a digital oscilloscope (Nicolet Technologies, Middleton, WI, USA). Neurone impalement was considered satisfactory when the recorded potential showed an abrupt and maintained deflection more negative than −40 mV and the neurone exhibited action potentials (APs) overshooting 0 mV. Only F-EPSPs that had an amplitude of 3 mV or greater were analysed. Membrane input resistance was calculated by Ohm's law from the data obtained by intracellular injection of hyperpolarizing current pulses (0.1 nA, 100 ms, 1 per 10 s) using a Grass S88 Stimulator (Grass Medical Instruments, Quincy, MA, USA). Electrical stimulation of the lumbar colonic nerve (0.5 ms pulses, 30–50 V) with bipolar platinum electrodes was used to evoke synaptic potentials.

During some electrophysiological experiments, Lucifer Yellow (LY, Sigma; 4% in 0.5 M LiCl) was injected intracellularly into IMG neurones using negative current pulses (1.0–1.5 nA, 200 ms, 4–5 Hz) for 10 min and ganglia were fixed and processed for immunostaining as described below.

PACAP27 and PACAP38 (Biochem Bioscience Inc., King of Prussia, PA, USA) were applied either by superfusion (500 nM in NKS) or by $N_2$ pressure microejection (pipette solution: 5 μM in NKS; 50–150 ms duration 'puffs'; Multi-Channel Picospritzer, General Valve Corp., Fairfield, NJ, USA) from a 10 μm diameter glass micropipette brought into close proximity (50–100 μm) to the impaled neurone. Maxadilan (a gift from Dr E. A. Lerner, Massachusetts General Hospital, Charlestown, MA, USA), an agonist for the PAC1-R (Moro & Lerner, 1997), was applied either by superfusion (500 nM in NKS) or by $N_2$ pressure microejection (pipette solution: 5 μM in NKS; 50–150 ms duration 'puffs'). In some experiments only the ganglion compartment of the two-compartment chamber was superfused with the PAC1-R antagonists PACAP6-38 (Bachem Bioscience Inc.; 500 nM in NKS) or the deleted (no. 25–41) peptide of maxadilan ('M65', a gift from Dr E. A. Lerner, Massachusetts General Hospital, Charlestown, MA, USA) (Eggenberger *et al.* 1999) or with VIP (Sigma; 500 nM in NKS). In other experiments, presynaptic transmitter release was suppressed by using either a modified low $Ca^{2+}$ (0.5 mM) high $Mg^{2+}$ (10 mM) Krebs solution or a Krebs solution containing the N-type $Ca^{2+}$ channel blocker ω-conotoxin GVIA TFA salt (Sigma; 1–10 μM in NKS). The nicotinic receptor antagonist, hexamethonium (Sigma; 100 μM in NKS), was used to block nAChRs.

### Measurement of release of PACAP peptides

In these experiments, four colon–IMG preparations were placed in a two-compartment organ bath as previously described (Ma & Szurszewski, 1996). Briefly, the IMGs were placed in a small central compartment (250 μl

volume) and their attached segments of distal colon (each 8–10 cm long) in a surrounding compartment. The ends of the segments were connected together with polyethylene catheters to allow for simultaneous distension. The ganglion compartment was perfused for 20 min with NKS containing 0.01% collagenase at 35–37°C. Thereafter and throughout the remainder of the experiment, NKS containing 0.2% bovine serum albumin and the protease inhibitor Trasylol (aprotinin, 500 U $ml^{-1}$, Miles, Inc., Kankakee, IL, USA) was used to perfuse the ganglion compartment to diminish breakdown of released peptide and facilitate recovery (Stapelfeldt & Szurszewski, 1989; Ma & Szurszewski, 1996). The experimental protocol consisted of two 2-min periods during which perfusion of the ganglion compartment was stopped to measure peptide release. During the first period, the colon was not distended (a control period). Then, after a 5 min washout period, the colon was distended during the second 2 min stopped flow period. Superfusates from 2 min stopped-flow periods were collected by aspiration and immediately frozen on dry ice. The protocol was repeated three times for each experiment and samples from respective periods were combined and preserved in a −80°C freezer for subsequent determination of PACAP peptides by competitive radioimmunoassay (PACAP27 radioimmunoassay kit RIK8922, Peninsula Laboratories, Inc., Belmont, CA, USA). The $IC_{50}$ value for PACAP27 in this assay was 17 pg per tube allowing sensitive detection of 1–128 pg per tube. The PACAP antiserum showed less than 1% cross-reactivity with VIP.

### Immunohistochemistry

Segments of the distal colon were cut open along the mesenteric attachment site, cleaned of their contents, placed in a Petri dish filled with chilled (4°C) NKS and pinned serosal surface down to the Sylgard-covered bottom of the dish (Dow Corning Corp., Midland, MI, USA). With the aid of a dissecting microscope, the mucosa, submucosa and circular muscle layer were carefully removed leaving the myenteric plexus attached to the longitudinal muscle layer. The preparations were incubated for 24 h at 22–24°C in tissue culture medium (HAM F-12, Sigma, St Louis, MO, USA) containing 80 $\mu$M colchicine (Sigma) and a 1% antibiotic–antimycotic solution (Sigma). The culture medium was constantly bubbled with a gas mixture containing 97% $O_2$ and 3% $CO_2$. After incubation, the tissue was washed with phosphate buffered saline (PBS; 0.1 M, pH 7.4) and fixed overnight with 4% phosphate buffered paraformaldehyde (PF) at 4°C and then rinsed in PBS. IMGs and DRGs were fixed overnight at 4°C, rinsed in PBS and then immersed in PBS containing 30% sucrose for 20–30 h at 4°C before freezing in isopentane at −50°C. Sections, 15–30 $\mu$m thick, were cut using a cryostat and thaw-mounted onto glass slides. IMGs containing LY-filled neurones were treated with colchicine as described above, fixed in PF, and immunostained as whole mount preparations. For immunostaining, tissues were first incubated for 1 h in PBS containing 10% normal goat or donkey serum (NS) and 0.3% Triton X-100 (blocking solution, BS) and then incubated for 1–2 days at 4°C with one of the following antibodies diluted in PBS containing 5% NS and 0.3% Triton X-100: rabbit polyclonal antiserum against PACAP27 (Peninsula Laboratories; 1 : 500–1 : 1000); rabbit polyclonal anti-serum against PACAP38 (Peninsula Laboratories; 1 : 500 to 1 : 1000); rabbit polyclonal antiserum against synthetic peptide corresponding to the C-terminal intracellular domain of PACAP type I receptor (PAC1-R, a gift from Dr A. Arimura, Japan Biomedical Research Laboratories, Belle Chasse, LA, USA; 1 : 1000), rabbit polyclonal antiserum against VIP (Laboratory Medicine and Pathology, Mayo Clinic, Rochester, MN, USA; 1 : 200); rat monoclonal IgG MAb35 to detect nAChRs (American Type Culture Collection, Rockville, MD, USA; 1 : 1200), and goat polyclonal anti-vesicular acetylcholine transporter (VAChT) antiserum (H-V007, Phoenix Pharmaceuticals, Inc., Belmont, CA, USA; 1 : 1000). PACAP27-LI, PACAP38-LI, PAC1-R-LI, VIP-LI, nAChR-LI and VACht-LI were revealed with appropriate secondary antibodies conjugated to Cy3 or Cy5 (Jackson Immuno-Research Laboratories, Inc., West Grove, PA, USA); diluted 1 : 100 in 2.5% NS containing 0.3% Triton X-100. Substitution of the various primary antibody solutions with PBS containing 5% NS and Triton X-100 only was used for a negative control. Additionally, in separate experiments, PACAP27 antibody preincubated with VIP (V3628, Sigma; 1 : 10) and PACAP38 Amide (H-8430, Bachem, Torrence, CA, USA; 1 : 10), and PACAP38 antibody preincubated with VIP (1 : 10) and PACAP27 (H-1172, Bachem 1 : 10) were also used as controls. After incubation in the secondary antibody solutions, tissues were rinsed in PBS, coverslipped in Gel/Mount™ (Biomeda Corp., Foster City, CA, USA) and stored at 4°C for subsequent imaging. Preincubation of PACAP27 antibody with PACAP38 ligand abolished immuno-staining as did preincubation of PACAP38 antibody with PACAP27 ligand. Thus, both antibodies recognized PACAP27 and PACAP38 in whole ganglia. Therefore, in this report, we will refer to PACAP-LI without reference to the specific form of PACAP. Immunostaining for PACAP-LI was specific because preincubation of PACAP antibodies with VIP did not affect PACAP27 or PACAP38 immunostaining.

### Confocal microscopy and three-dimensional imaging

Tissues were examined and imaged with a confocal laser scanning microscope (LSM 310 or 510, Carl Zeiss, Inc.,

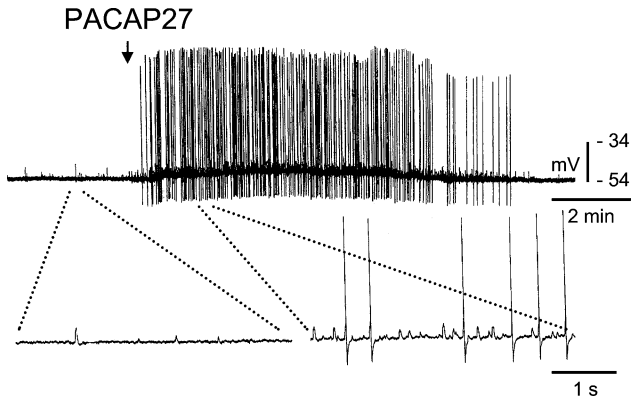


**Figure 1. Effect of PACAP27 on an IMG neurone that received ongoing excitatory synaptic input from the colon**
Top panel, a single 50–150 ms pressure application of PACAP27 (5 $\mu$M) evoked an intense and long lasting excitatory response accompanied by a marked increase in the frequency of F-EPSPs and APs and a slow depolarization of the membrane potential. Bottom panel shows portions of the recording on an expanded time scale to reveal individual post synaptic potentials.

Thornwood, NY, USA) equipped with a krypton/argon ion laser. To visualize LY-filled neurones, a laser wavelength of 488 nm and a band-pass filter of 535/35 nm were used. CY3 and CY5 were visualized with laser wavelengths of 568 nm and 633 nm, and optical filters of 585–615 nm and long-pass of 650 nm, respectively, were used. Images of LY-filled neurones, and surface

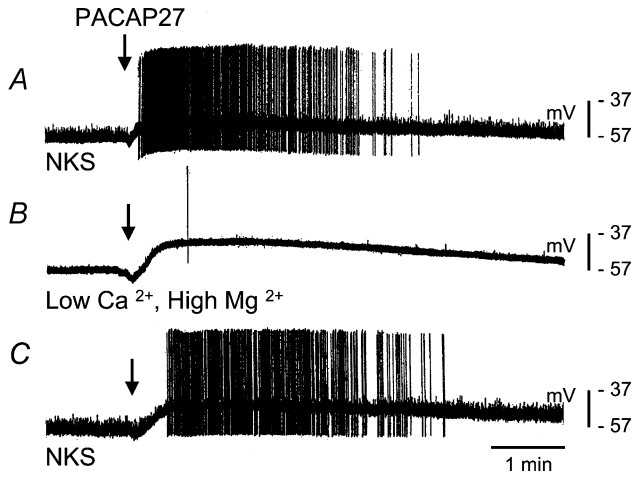


**Figure 2. Effect of PACAP27 on an IMG neurone (IMG–colon preparation) during superfusion of the ganglion with low $Ca^{2+}$, high $Mg^{2+}$ solution to block synaptic transmission**
*A*, a 100 ms pressure application of PACAP27 (arrow) to the ganglion depolarized the membrane and increased the frequency of F-EPSPs and APs. *B*, in the presence of a modified Krebs solution ($Ca^{2+}$ 0.5 mM, $Mg^{2+}$ 10 mM, 20 min) fast synaptic input to the neurone was markedly reduced. Upon pressure application (100 ms) of PACAP27 (arrow) there was a depolarization of similar amplitude and duration as in NKS but there was no increase in the frequency of fast synaptic potentials. *C*, upon washout with NKS (20 min), fast synaptic input and the response to application of PACAP27 were restored.

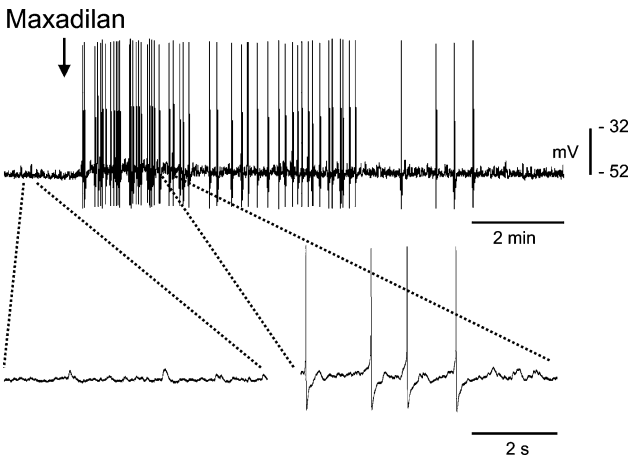


**Figure 3. Effect of maxadilan on electrical activity of IMG neurones**
Single pressure application (5 $\mu$M, 150 ms) of maxadilan (arrow) resulted in a slow membrane depolarization and increase in the frequency of F-EPSPs and APs. The bottom panel shows expanded time scales of the portions of the recording of the upper panel (dashed lines). These results show that maxadilan, a selective agonist of PAC1-R, mimics the action of PACAP27 on guinea pig IMG neurones.

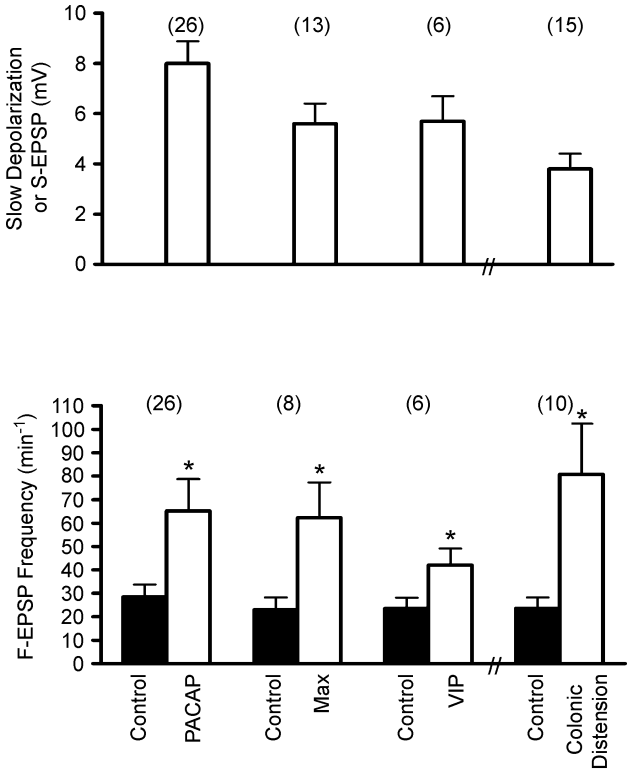


**Figure 4. Effect of direct application of PACAP27, maxadilan (Max), VIP and colonic distension on amplitude of slow depolarization, S-EPSP and frequency of F-EPSP in IMG neurones**
Values for the first three columns in the upper panel are for the amplitude of the peptide-evoked membrane depolarization whereas the fourth column is for the amplitude of the S-EPSP evoked by colonic distension. Control values are from measurements taken before application of the agonists or colonic distension. The number of experiments is shown in parenthesis (*indicates $P < 0.05$, paired $t$ test compared to corresponding control values).

distribution of PAC1-Rs, nAChRs, and putative synaptic contacts immunoreactive for PACAP, VIP, and VAChT were acquired in separate digital files for computer assisted three-dimensional reconstruction as previously described (Ermilov *et al.* 2000; Ermilov *et al.* 2003) using ANALYZE™ software (Biomedical Imaging Resource, Mayo Clinic and Foundation, Rochester, MN, USA). Thirty to 100 serial optical slices were acquired for each LY-filled neurone and reconstructed into an image consisting of voxels with an edge dimension ranging from 0.3 to 0.4 $\mu$m depending upon the magnification. To determine the surface area of the soma and visible portions of its processes, the software summed the voxel faces on the surface of the image and multiplied the number of faces by the surface area of each face. Voxels on the surface of the neuronal image that also contained signal from structures positive for PAC1-Rs and nAChRs were considered to contain putative receptors. Quantifying either the actual number or the surface area of the receptors could not be accomplished because of the size of the voxel was much larger than

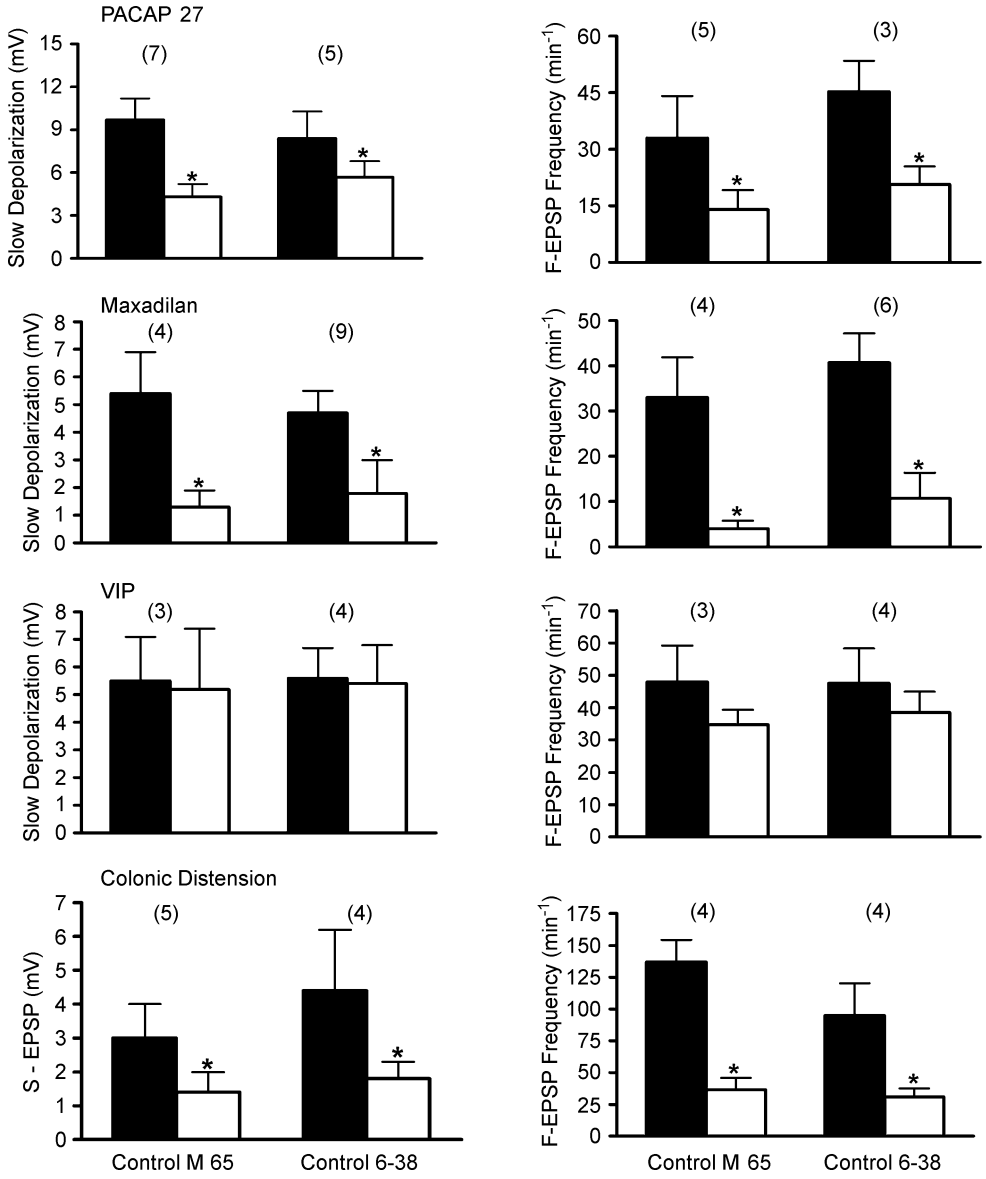


**Figure 5. Summary of the effect of preincubation (5–15 min) of the IMG with PAC1-R antagonists PACAP6-38 and M65 on the slow depolarization amplitude and F-EPSP frequency evoked in the IMG neurones by direct pressure application of PACAP27, maxadilan and VIP, and on the S-EPSP amplitude and F-EPSP frequency evoked in these neurones by colonic distension**

The number of experiments is shown in parentheses. Significantly different values ($P < 0.05$, paired $t$ test) compared to corresponding values in control (before the antagonists application) are marked with an asterisk.

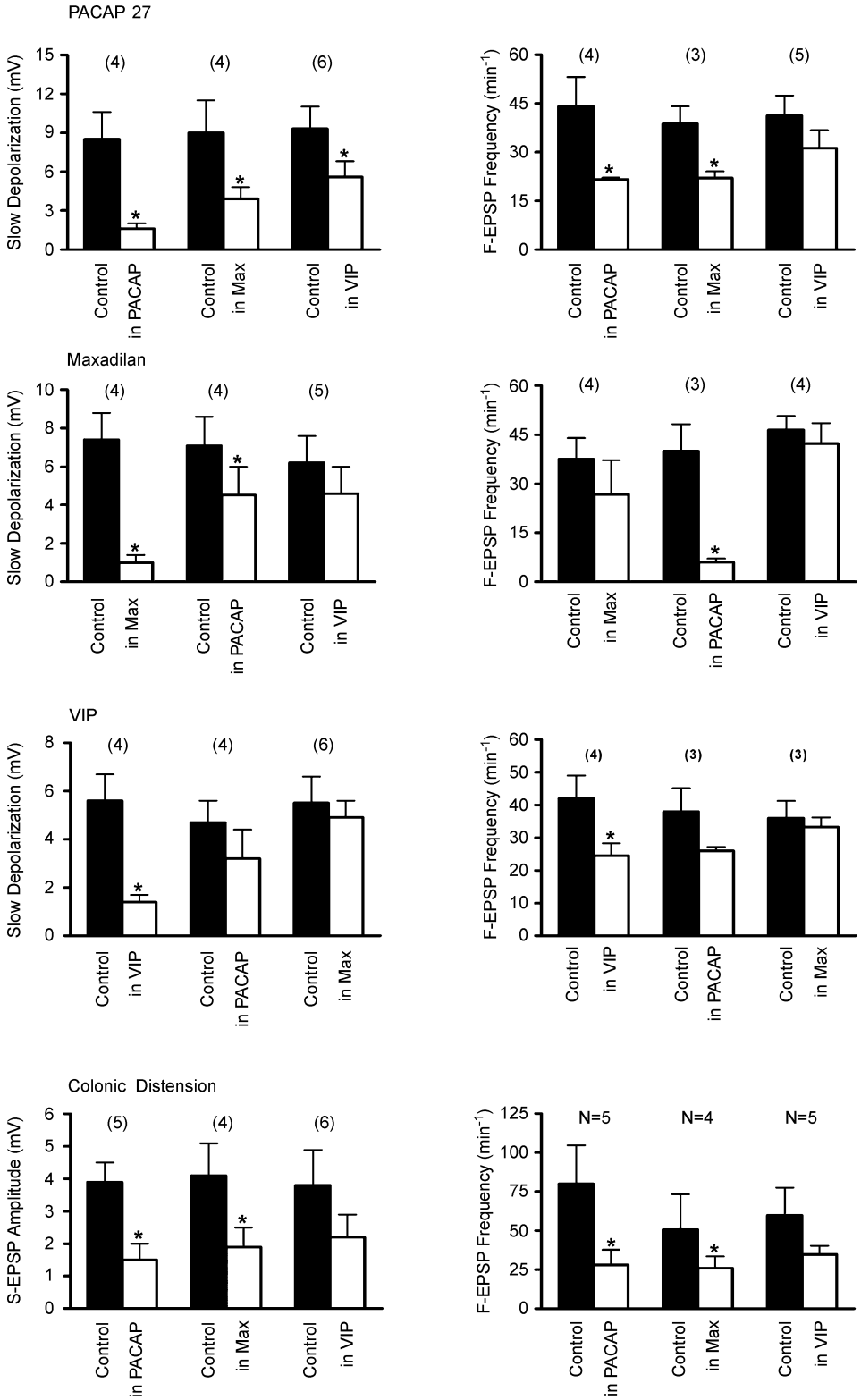


**Figure 6. Summary of the effect of preincubating the IMG (5–15 min) with PACAP27, maxadilan and VIP on depolarization, the S-EPSP amplitude, and on the F-EPSP frequency evoked in the IMG neurones by the direct pressure application of PACAP27, maxadilan and VIP and by colonic distension**

All recordings were made in 'colon–IMG' preparations. The number of experiments is shown in parentheses. Significantly different values ($P < 0.05$, paired $t$ test) compared to corresponding values in control are marked with an asterisk.

the actual size of the receptor. In other words since a receptor is many times smaller than the voxel size, there may be many receptors in the area represented by one voxel. To identify putative synaptic contacts, the neuronal image was expanded by one voxel creating a one voxel deep shell around the original image. Any voxels in the expanded area which also included signal from structures immunopositive for PACAP, VIP and VAChT were considered to contain potential synaptic contacts. Again, since the voxel size was significantly greater than the width of a synaptic cleft it was not possible to know whether the structure in the voxels was close enough to the neuronal membrane to be an actual synapse. Because of the resolution limitation, the amount of receptor or neuromodulator seen on a particular structure is reported as a percentage of that seen on the soma plus the visible processes. After reconstruction the image could be rotated for visual inspection of any surface and the location of the receptors and neuromodulators.

### Statistical analysis

Values are given as means ± S.E.M. Statistical significance was determined by Student's unpaired or paired $t$ tests and differences were considered statistically significant if $P < 0.05$.

## Results

### Effect of PACAP peptides

The resting membrane potential of IMG neurones when superfused with NKS was $-50.6 \pm 0.7$ mV (range: $-42$ to $-58$ mV; 63 cells in 43 preparations). When a segment of distal colon was left attached to the IMG (18 colon–IMG preparations), all 34 neurones tested exhibited ongoing F-EPSPs ($24.2 \pm 5.0\ \text{min}^{-1}$) and APs due to excitatory synaptic input from intestinofugal neurones, as previously described (Szurszewski & Miller, 1994). A single 50–150 ms pressure pulse application of PACAP27 evoked a slow depolarization of the membrane potential of $8.0 \pm 0.9$ mV amplitude (range: 3–19 mV; 26 cells; 16 preparations) that lasted 2–18 min and was accompanied by an increase in membrane input resistance ($57.8 \pm 4.8$ MΩ after compared to $49.9 \pm 3.9$ MΩ before PACAP application; 9 cells, 3 preparations, $P < 0.05$). The neurones also responded to PACAP27 with an intense discharge of APs and an increase in frequency of F-EPSPs ($28.5 \pm 5.3\ \text{min}^{-1}$ before PACAP27 application to $65.2 \pm 13.6\ \text{min}^{-1}$ after application; $P < 0.05$, $n = 26$). Figure 1 shows a representative response. In eight of the neurones tested, PACAP27 also increased the amplitude of the afterspike hyperpolarization to $16.0 \pm 1.0$ mV from $11.6 \pm 0.9$ mV in NKS ($P < 0.05$). PACAP38 had effects similar to those observed with PACAP27. A single pressure pulse application of PACAP38 (50–150 ms) evoked a slow membrane depolarization of $9.9 \pm 1.4$ mV in amplitude and $5.9 \pm 1.7$ min in duration (8 cells of 5 preparations). All eight neurones tested also responded with an intense discharge of APs, and an increase in the frequency of F-EPSPs ($45.8 \pm 5.2\ \text{min}^{-1}$ after compared to $20.8 \pm 3.0\ \text{min}^{-1}$ before PACAP38 application, $P < 0.05$). Although the mean membrane input resistance of $52.4 \pm 4.1$ MΩ after PACAP38 application was higher than the mean of $49.9 \pm 4.5$ MΩ before PACAP38, the change was not significant ($P > 0.05$, 5 cells, 4 preparations). Pressure pulse applications of normal Krebs solution (50–150 ms, $n = 5$) had no effect on F-EPSP and AP frequency.

In preparations of the IMG without an attached segment of colon, ongoing F-EPSP activity in IMG neurones was rarely observed when ganglia were superfused with NKS

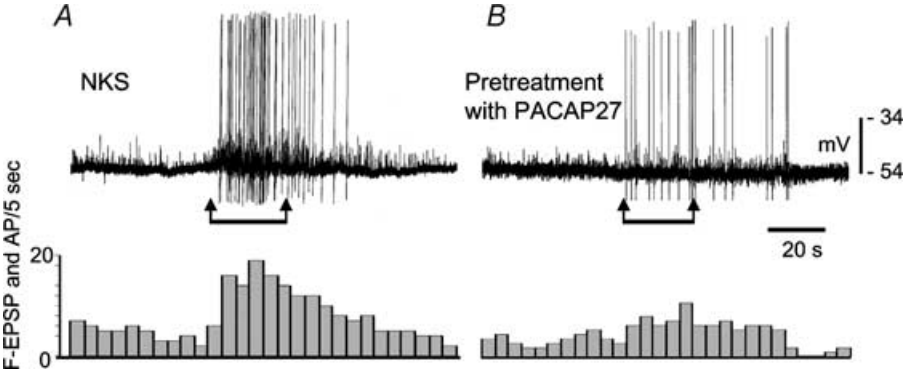


**Figure 7. Effect of desensitization of PAC1-Rs and VPAC-Rs on a single IMG neurone on colonic distension-evoked neuronal response**
*A*, control. *B*, after desensitization. Receptor desensitization was attained by ganglion preincubation for 20 min with PACAP27 (500 $\mu$M). Period of colonic distension of 10 cm $H_2O$ is marked with arrows. The bottom diagrams indicate the frequency of the F-EPSPs with amplitude greater then 3 mV and of the APs counted in 5 s bins from the electrical recordings in *A* and *B*. NKS, normal Krebs solution.

(34 cells, 16 preparations). However, F-EPSPs occurred immediately upon application of PACAP27 and PACAP38. The F-EPSPs were blocked by superfusion with the nicotinic receptor antagonist hexamethonium (100 $\mu$M in 6 of 6 cells tested in 4 IMGs). The slow depolarization evoked by the PACAP peptides in the same neurones was not significantly altered by hexamethonium ($7.6 \pm 1.6$ mV amplitude before compared to $7.0 \pm 1.0$ mV amplitude in the presence of hexamethonium, $P > 0.05$). These data suggested that PACAP27 and PACAP38 acted directly on IMG neurones to depolarize the membrane potential and indirectly via presynaptic sites. Because F-EPSPs in the IMG are nicotinic cholinergic (Szurszewski & Miller, 1994), the data suggested that both PACAP peptides facilitated nicotinic cholinergic transmission. The following experiments were done to test this hypothesis.

In colon–IMG preparations, superfusion of the IMG with a low $Ca^{2+}$ (0.5 mM), high $Mg^{2+}$ (10 mM) solution blocked ongoing F-EPSP activity as shown in Fig. 2, as well as F-EPSPs evoked by supramaximal (100 V, 0.5 ms) electrical stimulation of the lumbar colonic nerve (data not shown). Application of PACAP27 (50–150 ms) in the presence of the low $Ca^{2+}$, high $Mg^{2+}$ solution still evoked a depolarization of the membrane potential ($9.3 \pm 2.1$ mV, 7 cells compared to $8.0 \pm 0.9$ mV in NKS, 26 cells, 16 preparations, $P > 0.05$) and increased membrane input resistance ($59.2 \pm 6.8$ mΩ, 6 cells compared to $57.8 \pm 4.8$ mΩ in NKS; 9 cells, 3 preparations, $P > 0.05$). The duration of the depolarizing response to PACAP27 was similar under both conditions ($6.9 \pm 1.5$ min$^{-1}$ compared to $6.0 \pm 1.1$ min$^{-1}$ in NKS, 8 cells, 3 preparations, $P > 0.05$, paired $t$ test). However, as shown in Fig. 2*B*, the increase in the frequency of F-EPSPs evoked by PACAP27 seen in NKS was nearly completely abolished in the low $Ca^{2+}$, high $Mg^{2+}$ solution ($9.3 \pm 2.1$ min$^{-1}$ compared to $65.2 \pm 13.6$ min$^{-1}$ in NKS, $P < 0.05$). After washout of PACAP27 with NKS, the effect of PACAP on fast synaptic input was restored (Fig. 2*C*). PACAP27 was also tested in the presence of $\omega$-conotoxin (1–10 $\mu$M), a blocker of N-type $Ca^{2+}$ channels located on presynaptic terminals (Yahagi *et al.* 1998). Although the slow depolarizing response to PACAP27 was similar in NKS and in the presence of the blocker ($7.8 \pm 3.1$ mV, 3 cells, 2 preparations *versus* $8.0 \pm 0.9$ mV, 26 cells, 16 preparations, $P > 0.05$), the increase in F-EPSP frequency was nearly blocked by $\omega$-conotoxin ($6.3 \pm 2.6$ min$^{-1}$, $n = 3$, $P < 0.05$, paired $t$ test). Similar results were obtained using PACAP38.

### Effect of VIP

A single pressure pulse (50–150 ms) application of VIP (recordings not shown) evoked a slow depolarization of the membrane potential that ranged from 3 mV to 8.5 mV ($5.7 \pm 1.0$ mV, 6 cells, 3 preparations), lasted 0.5–3 min and increased AP discharge. VIP also increased the frequency of F-EPSPs ($42.0 \pm 7.1$ min$^{-1}$ compared to $23.5 \pm 4.6$ min$^{-1}$ in NKS; $P < 0.05$, paired $t$ test).

### Effect of the PAC1-R agonist maxadilan

Maxadilan, a recently discovered vasodilator peptide from the sand fly (*Lutzomyia longipalpis*), is a specific agonist with high potency for the PAC1-R in mammalian vascular smooth muscle (Moro & Lerner, 1997; Eggenberger *et al.* 1999). In colon–IMG preparations, a single (50–150 ms) pressure pulse application of maxadilan (500 nM) to the IMG evoked a slow depolarization in 13 of 18 IMG neurones tested (7 preparations). An example of the effect of maxadilan on membrane potential and on the occurrence of F-EPSPs and APs during intracellular recording is shown in Fig. 3. The slow depolarizing response ranged from 3.0 to 11.0 mV in amplitude ($5.6 \pm 0.8$ mV, 13 cells, 7 preparations) and from 20 s to 7.4 min in duration. The majority of neurones (9 of 13) also responded with an increase in AP frequency. Maxadilan also significantly increased F-EPSP frequency ($61.0 \pm 15.1$ min$^{-1}$ compared to $23.0 \pm 5.3$ min$^{-1}$ in NKS; $P < 0.05$, paired $t$ test). Figure 4 gives a summary of effects of PACAP27, maxadilan and VIP on the amplitude of the depolarizing response and the increase in the frequency of F-EPSPs in IMG neurones. Nineteen out of 24 neurones tested in five isolated IMGs also responded to maxadilan with an increase in F-EPSP frequency and AP discharge (data not shown). The amplitude of the S-EPSP and the increase in F-EPSP frequency due to colonic distension are shown in the right hand side of Fig. 4.

### Effect of the PAC1-R antagonist M65

M65, the deleted peptide (no. 25–41) of maxadilan, is a specific antagonist for the PAC1-R (Uchida *et al.* 1998; Gower *et al.* 2003). PACAP6-38 also is an antagonist to the PAC1-R (Harmar *et al.* 1998). We tested the effect of both antagonists on the response of IMG neurones to pressure pulse application of PACAP27, maxadilan and VIP in colon–IMG preparations. In these experiments, only the IMG compartment was superfused with NKS containing M65 (500 nM) or PACAP6–38 (500 nM). Both antagonists, tested in separate experiments, significantly reduced PACAP27- and maxadilan-evoked slow membrane depolarization and the increase in F-EPSP frequency (Fig. 5). For example, superfusion of the IMG with M65 reduced the maxadilan-evoked slow membrane depolarization from $5.4 \pm 1.5$ mV in NKS to $1.3 \pm 0.6$ mV, $P < 0.05$, paired $t$ test). The frequency of F-EPSPs was also significantly

reduced from $38.0 \pm 8.9\ \text{min}^{-1}$ in NKS to $4.0 \pm 1.8\ \text{min}^{-1}$ ($P < 0.05$, paired $t$ test) in the presence of M65 (Fig. 5). PACAP6-38 had effects similar to those observed with M65 (Fig. 5). These data support the hypothesis that the response to maxadilan and PACAP27 was mediated by PACAP preferring receptors (PAC1-R) located at presynaptic and postsynaptic sites. The depolarizing response and increase in F-EPSP frequency evoked by VIP, however, was not significantly affected by either M65 or PACAP6–38 (Fig. 5). Taken together, these data suggest that VPAC receptors as well as PAC1-Rs are also present in the guinea pig IMG and that VPAC receptors are located at presynaptic and postsynaptic sites.

We also examined the effect of M65 and PACAP6-38 on the response of IMG neurones to physiological levels of colonic distension (8–10 cm$H_2O$, 20–30 s). Superfusion of only the ganglion chamber with M65 (500 mM) or PACAP6–38 (500 mM) significantly reduced the amplitude of the S-EPSP ($1.4 \pm 0.6$ mV and $1.8 \pm 0.5$ mV, respectively, compared to $3.0 \pm 1.0$ mV and $4.4 \pm 1.8$ mV in NKS, respectively, $P < 0.05$, paired $t$ test), and the increase in F-EPSP frequency evoked by colonic distension ($36.5 \pm 9.4\ \text{min}^{-1}$ and $31.0 \pm 6.6\ \text{min}^{-1}$, respectively, compared to $137.0 \pm 17.4\ \text{min}^{-1}$ and $95.0 \pm 25.3\ \text{min}^{-1}$ in NKS, respectively, $P < 0.05$ paired $t$ test, Fig. 5), suggesting that the S-EPSP and increase in F-EPSP frequency were mediated in part by the release of PACAP peptides acting on PAC1-Rs. To further test these hypotheses, the effects of PACAP27, maxadilan and VIP were studied in colon–IMG preparations in which only the IMG was pretreated with one of the agonists to cause receptor desensitization. In these experiments, the ganglia were continuously superfused with NKS containing PACAP27 (500 nM), maxadilan (500 nM) or VIP (500 nM). In all neurones tested, superfusion with PACAP27, maxadilan and VIP initially caused a depolarization and an increase in F-EPSP frequency which was followed in the maintained presence of the agonist by a gradual repolarization to the membrane potential recorded before administration of the agonist and a return of F-EPSP frequency to the control level. The response to the agonist applied by a pressure pulse (50–150 ms) was once again tested while still recording from the same neurone. As expected, the response to a pressure pulse application of the same agonist that was continuously applied by superfusion was significantly reduced compared to the response evoked in NKS alone (Fig. 6). For example, superfusion of the IMG with maxadilan significantly reduced the amplitude of slow depolarization and the increase in frequency of S-EPSP evoked by a pressure pulse application of maxadilan ($1.0 \pm 0.4$ mV compared to $7.4 \pm 1.4$ mV in NKS, and $26.8 \pm 10.5\ \text{min}^{-1}$ compared to $37.5 \pm 6.5$ in NKS, respectively, $P < 0.05$, paired $t$ tests, Fig. 6). In addition, we found that pretreatment with maxadilan significantly reduced the amplitude and duration of the slow depolarization in response to PACAP27 ($3.3 \pm 0.9$ mV compared to $9.0 \pm 2.5$ mV in NKS and $22.0 \pm 2.0\ \text{min}^{-1}$ compared to $38.7 \pm 5.3\ \text{min}^{-1}$ in NKS, respectively, $P < 0.05$, paired $t$ tests, Fig. 6). Pretreatment with PACAP27 significantly reduced the response to maxadilan ($4.5 \pm 1.5$ mV compared to $7.1 \pm 1.5$ mV in NKS and $6.0 \pm 1.2\ \text{min}^{-1}$ compared to $40.0 \pm 8.3\ \text{min}^{-1}$ in NKS, respectively; $P < 0.05$, paired $t$ tests, Fig. 6). In contrast, while pretreatment with VIP significantly reduced the response to PACAP27, it did not significantly reduce the response to pressure application of maxadilan (Fig. 6). Furthermore, desensitization to PACAP27 and maxadilan had no significant effect on the depolarizing response and the increase in F-EPSP frequency due to the action of VIP (Fig. 6). In three experiments (4 cells tested) where the IMG was continuously superfused for 10–15 min with

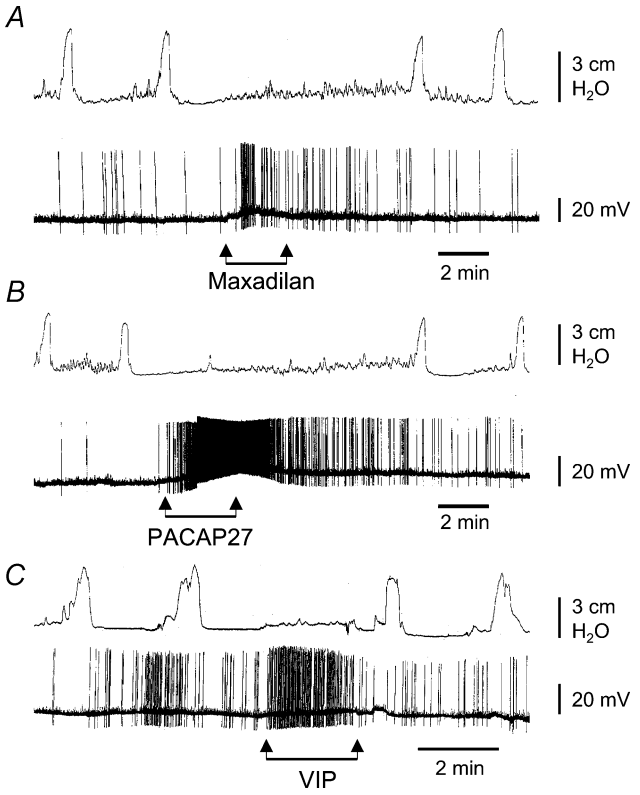


**Figure 8. Effect of superfusing the IMG with maxadilan (*A*), PACAP27 (*B*) and VIP (*C*) on intracellularly recorded electrical activity of IMG neurones (lower traces) and intraluminal pressure of the attached colonic segment (upper traces)**
Note that application of maxadilan and PACAP27 evoked neuronal activation that either strongly depressed or abolished colonic contractions. In 2 out of 11 experiments, application of PACAP27 also caused relaxation (decrease in resting pressure) of the colon segment (not shown). Application of VIP, which also activated the IMG neurones, abolished colonic motility in 2 out of 9 experiments. In the other 7 experiments VIP either only slightly depressed or did not cause any changes in the amplitude and frequency of colonic contractions (not shown in this figure). All agents were used at 500 nM, diluted in NKS.

**Table 1. Effect of superfusion of the IMG with PACAP27, maxadilan and VIP on colonic motility**

| | Depression of the amplitude of spontaneous contractions | Inhibition of the frequency of spontaneous contractions | No effect on motility |
|---|---|---|---|
| PACAP27 | 5/11 | 6/11 | 0/11 |
| Maxadilan | 7/10 | 3/10 | 0/10 |
| VIP | 2/9 | 2/9 | 5/9 |

Values are numbers of preparations with the particular effects caused by superfusion with the peptides over the total number of the preparations tested.

Krebs solution containing both maxadilan (500 mM) and VIP (500 mM) to desensitize PAC1-R and VPAC receptors, pressure pulse application (50–150 ms) of PACAP27 failed to evoke a membrane depolarization and failed to alter F-EPSP frequency. When considered together, the results of the above pharmacological experiments provide additional data to support the notion that PAC1-Rs and VPAC receptors are located at presynaptic and postsynaptic sites in the IMG, that maxadilan acts only at PAC1-Rs, and that the response to PACAP27 appears to be mediated through both PAC1-Rs and VPAC receptors.

We also tested the effect of pretreatment of only the IMG with PACAP27, maxadilan or VIP on the response of IMG neurones to colonic distension (8–10 $cmH_2O$, 20–30 s). As summarized in Fig. 6, desensitization to PACAP27 and maxadilan significantly reduced the amplitude of the S-EPSP ($1.5 \pm 0.5$ mV compared to $3.9 \pm 0.6$ mV in NKS and $1.9 \pm 0.6$ mV compared to $4.1 \pm 1.0$ mV in NKS, respectively, $P < 0.05$, paired $t$ test) and the increase in F-EPSP frequency ($28.0 \pm 9.7\ min^{-1}$ compared to $80.0 \pm 24.7\ min^{-1}$ in NKS and $26.0 \pm 7.4\ min^{-1}$ compared to $50.8 \pm 22.6\ min^{-1}$ in NKS, respectively, $P < 0.05$, paired $t$ test). An example of the effect of pretreatment with PACAP27 is shown in Fig. 7. Desensitization to VIP on the other hand had no significant effect on colonic distension-evoked responses in IMG neurones (Fig. 6).

### Effect of PACAP27, maxadilan and VIP on colonic intraluminal pressure

The lumbar colonic nerve contains axons of IMG sympathetic neurones that inhibit colonic motor activity (Furness & Costa, 1987; Szurszewski & Miller, 1994). We hypothesized that the increase in excitability of IMG neurones during superfusion of the ganglion with agonists to PAC1 or VPAC receptors would increase sympathetic outflow to the colon and inhibit colonic contractions. This notion was tested in colon–IMG preparations in which colonic intraluminal pressure was monitored during superfusion of only the IMG with PACAP27, maxadilan or VIP (each 500 nM). Intracellular recordings were made from single IMG neurones as a way of assessing the effect of the peptides on IMG neurones. During control periods before superfusion of one of the peptides, phasic increases in colonic intraluminal pressure ($4.3 \pm 0.2\ cmH_2O$) occurred at a frequency of $0.3\ min^{-1}$. In 7 of 10 experiments, superfusion of only the IMG with maxadilan either significantly reduced the amplitude of the phasic increases in pressure ($1.5 \pm 0.3\ cmH_2O$) or completely abolished their occurrence. Superfusion with PACAP27 abolished phasic colonic contractions in 6 of 11 experiments and significantly reduced the amplitude of contractions in the remaining five experiments ($2.7 \pm 0.5\ cmH_2O$ compared to $4.6 \pm 0.9\ cmH_2O$ in NKS, $P < 0.05$, paired $t$ test). A representative example of the effect of each of these peptides is shown in Fig. 8. VIP abolished phasic contractions in 2 of 9 experiments and significantly reduced their amplitude in two experiments ($2.5 \pm 0.5$ cm $H_2O$ compared to $4.2 \pm 1.0\ cmH_2O$ in NKS). There was no significant change in the remaining five experiments. Table 1 gives a summary of the effects of the three peptides on colonic contractions.

### Release of PACAP27

In 9 of 9 experiments, there was a detectable release of PACAP peptides during basal conditions ($7.0 \pm 1.0$ pg per tube). In 8 of 9 experiments, colonic distension (20–25 $cmH_2O$) increased the amount of PACAP peptides recovered in the IMG ($8.2 \pm 1.0$ pg per tube, $P < 0.05$, paired $t$ test).

### PACAP-immunoreactivity

PACAP-LI was detected in the IMG, attached nerve trunks, colonic myenteric ganglia and DRG of $L_2$ and $L_3$. Each of the regions was examined in preparations from five different animals. The results were similar in all five animals. Data from one animal are shown in Fig. 9. Varicose nerve fibres with PACAP-LI surrounded cell bodies in the IMG (Fig. 9*A*) whereas cell bodies of IMG neurones were not immunopositive for PACAP. Intense PACAP-LI was found in nerve fibres in the intermesenteric (Fig. 9*B*), hypogastric (Fig. 9*C*), and lumbar colonic (Fig. 9*D*) nerves whereas fewer nerve fibres containing PACAP-LI were detected in the inferior splanchnic nerves (Fig. 9*H*). Approximately 15% of neurones in DRG of $L_2$ and $L_3$ had PACAP-LI (Fig. 9*I*). The mean somal diameter ($29.5 \pm 1.8\ \mu m$, $n = 18$) for dorsal root ganglion neurones with PACAP-LI was significantly ($P < 0.05$) smaller compared to $36.7 \pm 2.1\ \mu m$ ($n = 23$) for non-PACAP-immunoreactive neurones. In colonic

myenteric ganglia, nerve fibres with PACAP-LI surrounded non-immunoreactive cell bodies (Fig. 9*E*). A small subset of myenteric ganglion neurones contained PACAP-LI (Fig. 9*F* and *G*). Although a shape-based classification of PACAP-positive neurones could not be easily made because of the dense network of intensely stained fibres passing in the vicinity of these neurones, it was apparent that some had a single long axon and a few short

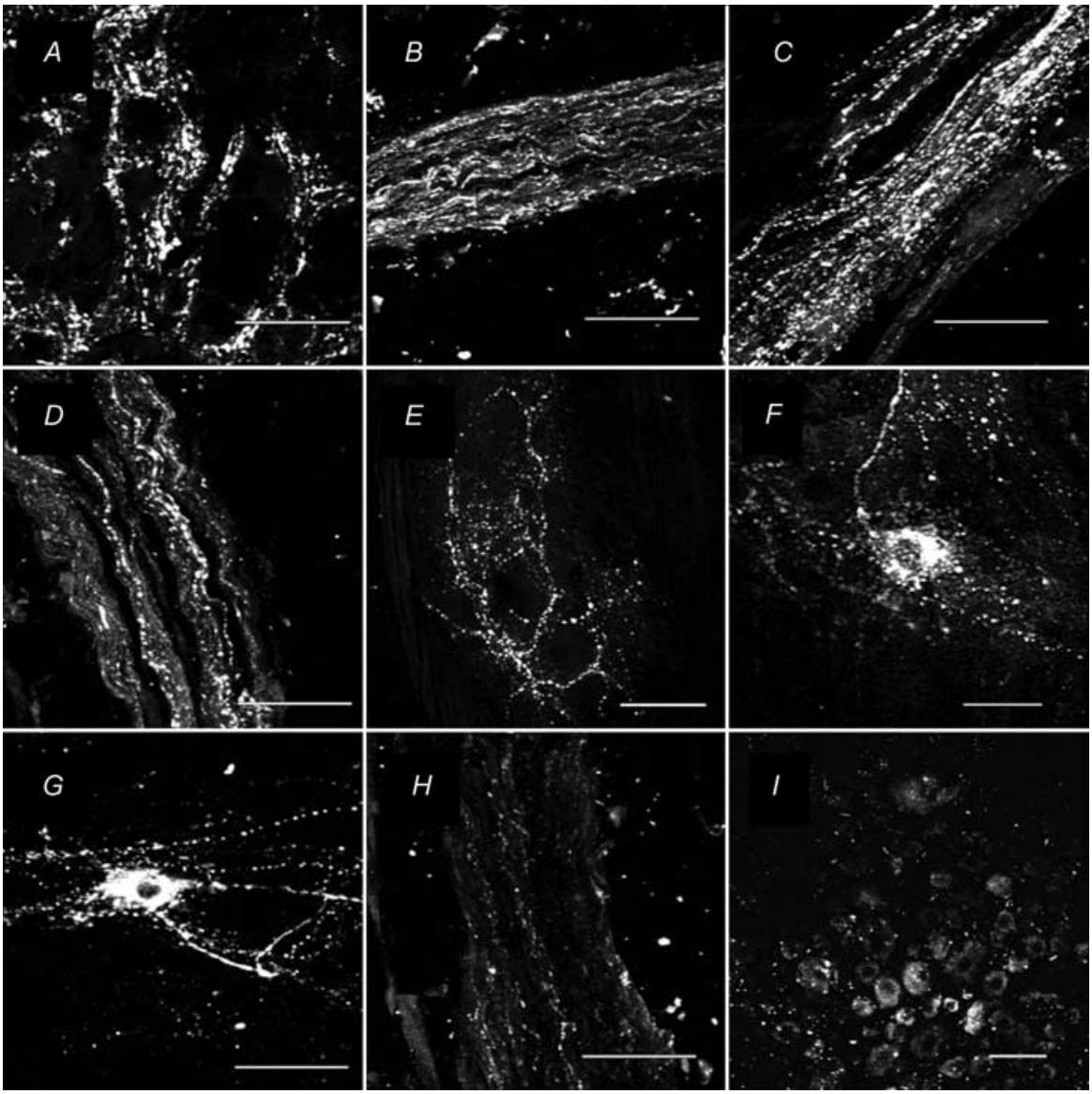


**Figure 9. Micrographs showing immunohistochemical staining for PACAP-LI in the guinea pig**
*A*, inferior mesenteric ganglion; *B*, intermesenteric nerve trunk; *C*, hypogastric nerve trunk; *D*, lumbar colonic nerve trunk; *E–G*, myenteric ganglia of the distal colon; *H*, inferior splanchnic nerves; and *I*, $L_2$ dorsal root ganglion. Note the varicose appearance of PACAP-LI in the IMG (panel *A*). No cell bodies containing PACAP-LI were found in the IMG. In the lumbar colonic, hypogastric and intermesenteric nerves (panels *B–D*) there were numerous nerve fibres containing PACAP-LI. Only a few PACAP-LI nerve fibres were found in the inferior splanchnic nerves (panel *H*). A small number of cell bodies with PACAP-LI were found in the dorsal root ganglion (panel *I*). In the myenteric plexus of the colon (panel *E*), there was a dense network of nerve fibres containing PACAP-LI and occasional cell bodies of myenteric neurones also were stained. The shape-based classification of these neurones was unclear because of the dense network of intensely stained nerve fibres passing in the vicinity of the ganglion neurones. However, some of the neurones resembled Dogiel type I neurones having a single long axon and a few short dendrites (panel *F*) and some resembled Dogiel type II neurones having a smooth cell body and several long processes (panel *G*). The IMG, DRG and nerves were frozen sections (15 $\mu$m thick) and the myenteric plexus preparations were whole-mounts. Scale bars are 50 $\mu$m.

dendrites resembling Dogiel type I neurones (Fig. 9*F*), whereas others had a smooth cell body with two or more long processes resembling Dogiel type II neurones (Fig. 9*G*).

### Spatial distribution of PACAP-LI presynaptic boutons and PAC1-R-LI synapses

Three-dimensional reconstruction of LY-filled IMG neurones and superimposition of putative synaptic boutons containing PACAP-LI adjacent to the neurone are shown in Fig. 10*A*. Of six IMG neurones studied the mean total membrane surface area was $33\,540 \pm 2390\ \mu m^2$, the mean surface area of the soma was $5390 \pm 1040\ \mu m^2$, and the mean surface areas of the primary, secondary and tertiary processes were $11\,990 \pm 2360\ \mu m^2$, $10\,490 \pm 1270\ \mu m^2$ and $4470 \pm 1480\ \mu m^2$, respectively. The number of voxels containing PACAP signal and located within the dimension of one voxel from the neuronal surface (voxels that contained LY) membrane were counted and compared for the various parts of neurone including the cell body and visible processes using methods previously described (Ermilov *et al.* 2003). The majority ($54.0 \pm 9.4\%$) of these regions of contact were distributed along the secondary and tertiary dendrites (Table 2). The distribution of PAC1-Rs on the surface membrane of IMG neurones was assessed by counting the number of voxels comprising the neuronal membrane which were also immunopositive for PAC1-Rs. Cell surface-associated sites of PAC1-R-LI appeared as bright punctate patches or clusters covering the cell body and neuronal processes (Fig. 10*B*). The majority ($66.7 \pm 4.9\%$) of PAC1-R-LI sites were also distributed on the surface of the secondary and tertiary processes (Table 2).

### Spatial distribution of VIP-LI

The distribution of putative VIP-LI presynaptic terminals was measured in the same manner as the distribution of PACAP-LI on the surface of the IMG neurones. The putative terminals had a distribution similar to PACAP-LI (Fig. 11*A*, Table 2) with the majority of VIP-LI apposition on the secondary and tertiary processes ($55.9 \pm 5.7\%$).

### Spatial distribution of nAChRs and VAChT

Cell surface-associated sites of MAb35 immunoreactivity (putative nAChRs) were quite uniformly distributed on the surface of neuronal cell body and processes (Fig. 11*C*, Table 2); however, the majority of immunoreactive sites ($54.5 \pm 6.1\%$, $n = 6$) were found on the secondary and tertiary processes of IMG neurones. VAChT is required for the transport of ACh from the cytoplasm into synaptic vesicles. Thus, the spatial distribution of VAChT-LI sites is a marker of the presynaptic nerve endings containing ACh and the spatial distribution of VAChT-LI presynaptic sites

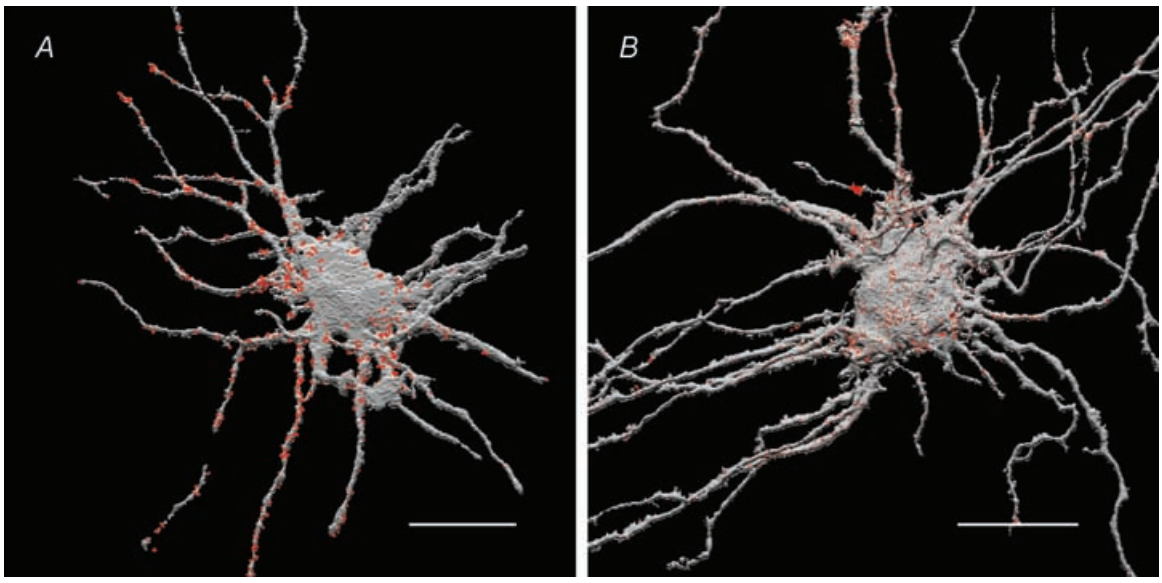


**Figure 10. Spatial (3-D) distribution of presynaptic PACAP-LI (*A*) and neuronal PAC1-R-LI (*B*) on IMG neurones**

The IMG neurones were intracellularly injected with LY fluorescent dye and the preparations were subsequently immunostained with appropriate antibodies visualized with either Cy3 or Cy5 fluorescent dyes. Preparations were imaged with confocal microscope and the images were volume reconstructed and superimposed using ANALYZE™ software (see Methods for details). Voxel counting revealed that the majority ($54.0 \pm 9.4\%$, $n = 6$ neurones) of PACAP-LI appositions (coloured red) and the majority ($66.7 \pm 4.9\%$, $n = 7$ neurones) of PAC1-R-LI (coloured red) were distributed along the secondary and tertiary processes of IMG neurones (coloured grey). Scale bars, 50 $\mu$m.

**Table 2. Spatial distribution of immunoreactivity reported as a percentage of surface membrane voxels**

| | | Processes | | |
|---|---|---|---|---|
| | Soma | Primary | Secondary | Tertiary |
| PACAP ($n = 6$) | $10.1 \pm 3.4$ | $35.9 \pm 7.4$ | $32.1 \pm 6.0$ | $21.9 \pm 9.1$ |
| PAC1-R ($n = 7$) | $18.8 \pm 3.5$ | $12.7 \pm 2.3$ | $35.3 \pm 6.1$ | $33.3 \pm 6.0$ |
| VIP ($n = 7$) | $21.3 \pm 4.9$ | $22.8 \pm 2.9$ | $27.4 \pm 4.7$ | $28.5 \pm 7.1$ |
| nAChR ($n = 6$) | $23.6 \pm 5.6$ | $21.9 \pm 2.8$ | $25.8 \pm 5.3$ | $28.7 \pm 4.8$ |
| VAChT ($n = 3$) | $14.5 \pm 8.3$ | $21.7 \pm 3.1$ | $36.8 \pm 7.6$ | $27.0 \pm 8.2$ |

Neuronal receptor regions were defined as surface membrane voxels that also contained immunoreactivity for receptor antibodies. Presynaptic nerve endings were defined as external structures immunopositive for PACAP, VIP VAChT that were within 1 voxel dimension of the neuronal surface membrane.

should match the postsynaptic distribution of putative nAChRs. In fact, as with the nAChR-LI, the VAChT-LI sites also were mostly distributed along secondary and tertiary processes of the IMG neurones ($63.8 \pm 6.9\%$, Fig. 11*B*). Values for the spatial distribution of MAb35-IR and VAChT-LI are shown in the Table 2.

Immunoreactivity for nAChRs was also observed in intracellular sites of LY-filled IMG neurones (Fig. 11*D*). Approximately 30% of the total immunoreactivity was found on the cell surface and 70% in intracellular sites. It is likely that the nAChR-LI observed inside LY-filled neurones was associated with intracellular organelles during biosynthesis and trafficking of nAChRs as in guinea pig myenteric neurones (Kirchgessner & Liu, 1998) and chick CNS neurones (Jacob *et al.* 1986). In summary, the quantitative data obtained in these volume reconstructed three-dimensional images show that putative presynaptic structures containing PACAP- and VIP-LI were broadly distributed along the dendrites of IMG neurones, and that the surface membrane of the neurones, especially of the dendrites, had regions immunopositive for PAC1-Rs and nAChRs.

## Discussion

The results of this study provide pharmacological, physiological and immunohistochemical data and three-dimensional quantitative imaging to support the hypothesis that PACAP in the guinea pig IMG is a modulator of the colon–IMG reflex loop. PACAP-LI was found in varicose nerve fibres surrounding IMG neurones, was released in the IMG during physiological levels of colonic distension, acted presynaptically to enhance the level of nicotinic cholinergic transmission, and acted directly on IMG neurones to increase membrane excitability and action potential frequency. The resulting increase in output firing frequency of IMG neurones inhibited colonic motility. The effects of PACAP were mediated by the PACAP-specific receptor PAC1, which binds PACAP with 1000-fold greater affinity than VIP, and by the VPAC receptors that have nearly equal affinity for VIP and PACAP (Pisegna & Wank, 1993; Harmar *et al.* 1998; Vaudry *et al.* 2000).

The dense network of varicosities with PACAP immunoreactivity surrounding IMG neurones originated from outside the ganglion, as no IMG neurones containing PACAP-LI were found. One source of the PACAP immunoreactive fibres in the IMG was from the myenteric ganglia of the distal colon as the lumbar colonic nerves were positive for PACAP-LI and some of the myenteric ganglion neurones that were immunoreactive for PACAP had a morphology characteristic of intestinofugal afferent neurones (IFANs) (Christofi & Wood, 1993; Lomax *et al.* 1999; Ermilov *et al.* 2003). The PACAP-LI found in the inferior splanchnic nerves and in small $L_2$ and $L_3$ DRG neurones indicates that other centrifugal pathways also supply IMG neurones with PACAP. Thus, intestinofugal colonic myenteric neurones and collaterals of spinal afferent neurones both appear to be the source of PACAP in the guinea pig IMG. Our immunohistochemical results confirm previous findings regarding the presence of PACAP peptides in myenteric neurones of the guinea pig intestine (Arimura, 1992; Portbury *et al.* 1995) and confirm previous observations that PACAP peptides are present in nerve fibres in the guinea pig IMG (Portbury *et al.* 1995). The present results are also in agreement with previous observations that PACAP peptides are present in dorsal root ganglion neurones (Portbury *et al.* 1995; Dun *et al.* 1996). PACAP-LI nerve fibres were also found in the present study in the intermesenteric and hypogastric nerves, raising the possibility that a subpopulation of PACAP-containing enteric ganglion neurones in the small intestine and rectum, respectively, send their axons to IMG neurones.

The effect of exogenously applied PACAP27 and PACAP38 to directly excite IMG neurones is similar to the direct effect of PACAP27 and PACAP38 seen in guinea pig myenteric and pancreatic ganglion neurones (Christofi &

Wood, 1993; Kirchgessner & Liu, 2001), canine gallbladder neurones (Mizumoto *et al.* 1992), rat sympathetic preganglionic neurones (Lai *et al.* 1997), cultured rat sympathetic ganglion neurones (May *et al.* 1998) and substance P/acetylcholine-containing rat myenteric ganglion interneurones (Grider, 1998). In contrast to the increase in membrane conductance to a non-selective cation current seen in rat superior cervical ganglion neurones (May *et al.* 1998) and guinea pig intracardiac ganglia neurones (Braas *et al.* 1998), PACAP27 and PACAP38 increased membrane input resistance in IMG neurones. Exogenously applied PACAP27 and

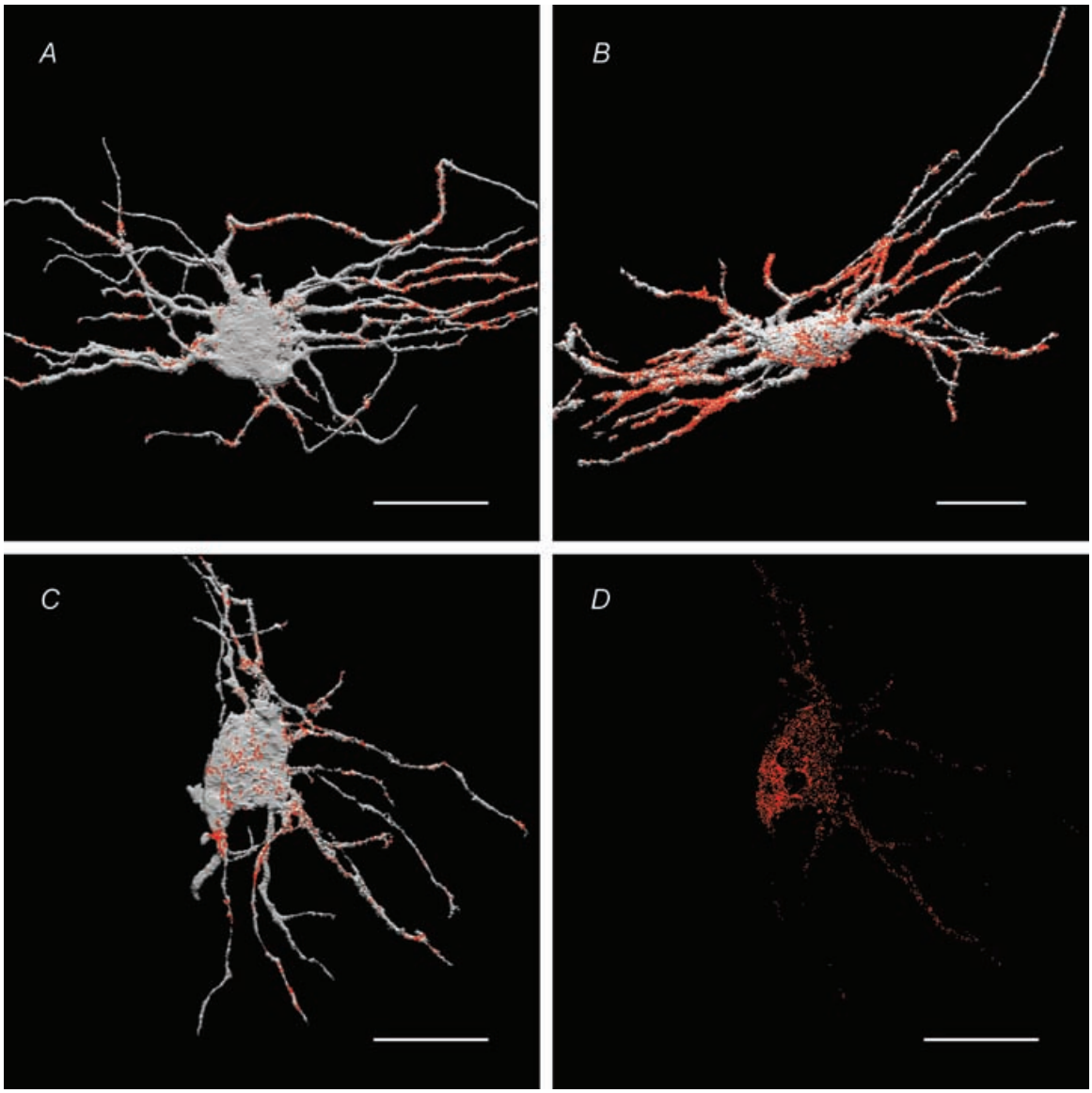


**Figure 11. Spatial (3-D) distribution of presynaptic VIP-LI and VAChT-LI appositions (*A* and *B*, respectively) on IMG neurones, and neuronal MAb35 immunoreactivity (putative nAChRs) on the surface (*C*) and inside the same neurone (*D*)**

IMG neurones were intracellularly injected with LY, immunostained with appropriate antibodies, visualized with either Cy3 or Cy5, and imaged using a confocal microscope. The images of the LY-filled neurones (coloured grey) and associated immunoreactive sites (coloured red) were volume reconstructed and superimposed using ANALYZE$^{TM}$ software (see Methods for details). Note that the majority of VIP-LI presynaptic endings (55.9 $\pm$ 5.7% of the total neurone-associated VIP LI-containing structures) were on secondary and tertiary dendritic branches of the neurone. Note that a majority of VAChT-LI (marker of the presynaptic ACh-containing terminals) and majority of MAb35 sites (marker of the nAChRs) were also found on secondary and tertiary dendrites (see Table 2 for quantification). The presence of MAb35-LI sites within the IMG neurone (panel *D*) most likely represents nAChR subunits associated with intracellular organelles during biosynthesis and trafficking of nAChRs (Ermilov *et al.* 2003). Scale bars, 50 $\mu$m.

PACAP38 also increased the frequency of F-EPSP activity. The increase in F-EPSP activity was due to release of acetylcholine from presynaptic endings because the increase was blocked by hexamethonium, $\omega$-conotoxin, and a low calcium–high magnesium solution which are known to block synaptic transmission in the IMG and other sympathetic ganglia (Szurszewski & Miller, 1994; Yahagi *et al.* 1998). Presynaptic effects of PACAP27 and PACAP38 also have been observed in the rat hippocampus (Masuo *et al.* 1993), guinea pig cardiac ganglia (Braas *et al.* 1998), atrial cholinergic neurones in the guinea pig (Seebeck *et al.* 1996), the guinea pig myenteric plexus (Katsoulis *et al.* 1993) and the opossum internal anal sphincter (Rattan & Chakder, 1997). PACAP27 and PACAP38 also increase synaptic transmission in the anterior pituitary (Rawlings & Hezareh, 1996) and act on vagal efferent nerves to induce gastric contraction (Onaga *et al.* 1998) and pancreatic enzyme secretion (Onaga *et al.* 1997). The substantial increase in excitability of guinea pig IMG neurones evoked by PACAP is all the more impressive because PACAP also increased the amplitude of the afterspike hyperpolarization, which would tend to decrease AP frequency.

The pharmacological experiments done in the present study suggest that both the postsynaptic and presynaptic actions of exogenously added and endogenously released PACAP were mediated through PAC1-Rs and VPAC receptors. The PAC1-R antagonist PACAP6-38 and M65, a specific antagonist of PAC1-Rs (Uchida *et al.* 1998; Tatsuno *et al.* 2001), blocked the depolarizing response and increase in F-EPSP activity due to exogenously added PACAP27 and PACAP38 and blocked colonic distension-induced S-EPSPs as well as the increase in frequency of F-EPSPs. Additional evidence supporting a role for PAC1-Rs comes from the observation that maxadilan, a specific agonist for PAC1-Rs (Moro & Lerner, 1997; Uchida *et al.* 1998; Eggenberger *et al.* 1999), mimicked the response to exogenously added PACAP27 and PACAP38 and that the effect of maxadilan was blocked by M65. The effect of PACAP27 and PACAP38 was partially but not significantly reduced during desensitization to VIP suggesting that the effect of the PACAP peptides was also mediated in part by VPAC receptors.

Desensitization of IMG neurones due to the prolonged application of VIP also significantly reduced the depolarizing response and increase in F-EPSP activity due to pressure pulse application of VIP. Since the PAC1-R has a low affinity for VIP (Harmar *et al.* 1998), it seems reasonable to conclude that the effect of VIP was mediated by VPAC receptors. Our study was not designed to determine whether the effect was mediated by VPAC1 or VPAC2 receptors, or both. When all of the pharmacological data are considered together, it seems reasonable to conclude that PAC1-Rs and VPAC receptors are present on presynaptic cholinergic nerve terminals and postsynaptically on IMG neurones. The superior cervical ganglion (May *et al.* 1998), a sympathetic ganglion, appears to express preferentially the PAC1-R (May & Braas, 1995; May *et al.* 1998), but that does not appear to be the case for the guinea pig IMG.

The finding that activation of PAC-1Rs and VPAC receptors increases the frequency of synaptic discharge onto IMG neurones raises two possibilities: (1) that not every action potential that invades a presynaptic terminal which innervates IMG neurones causes acetylcholine release in the absence of PAC1 or VPAC receptor activation, or (2) that activation of PAC-1Rs or VPAC receptors can cause transmitter release in the absence of presynpatic action potentials. Further experiments will be required to distinguish between these two possibilities.

The present findings that physiological levels of colonic distension released PACAP-LI in the IMG provide direct evidence that PACAP peptides are present in colonic mechanosensory IFANs and that PACAP peptides, like VIP, function physiologically as an excitatory neuromodulator in the guinea pig IMG (Szurszewski *et al.* 2002).

Regarding the spatial distribution of putative PACAP-, VIP- and acetylcholine-containing synaptic endings on single IMG neurones, we are not aware of any previous studies on the three-dimensional spatial distribution of putative synaptic contacts in peripheral autonomic ganglion neurones in whole mount preparations. The results of this study have identified a number of features of the spatial distribution of peptidergic and cholinergic synaptic regions that are likely to have an influence on the basic function of IMG neurones and on the overall performance of the colon–IMG reflex. More than 70% of the putative presynaptic structures were found apposed to the dendritic membrane, a structural arrangement which supports the notion based on electrophysiological data that the majority of synaptic inputs in IMG neurones occur on dendrites (Szurszewski & Miller, 1994). The present study also shows an uneven regional distribution of PAC1-Rs and nAChRs on IMG neurones with the greatest amount of both receptors on secondary and tertiary dendrites. Approximately 75% of the surface membrane voxels of IMG neurones containing signal for MAb35 and for the PACAP receptor were distributed on the dendrites. The majority of PACAP and VIP immunoreactive terminals were also distributed along secondary and tertiary dendritic branches. This similarity in the spatial distribution of putative nicotinic and peptidergic synaptic regions provides a structural basis whereby the efficacy of fast cholinergic nicotinic transmission can be modulated by the increase in membrane input resistance by VIP (Love & Szurszewski, 1987) and PACAP as shown in this study. The similarity in spatial distribution of cholinergic and peptidergic synaptic regions is consistent with previous immunohistochemical

studies showing colocalization of acetylcholine and neuropeptides in projections of intestinofugal neurones to IMG neurones in the guinea pig (Messenger & Furness, 1993).

In conclusion, the presence of PACAP-containing nerve endings in the guinea pig IMG suggests that release of PACAP peptides in the IMG reflexly alters colonic motility by modulating ganglionic transmission in the IMG.

## References


Arimura A (1992). Pituitary adenylate cyclase activating polypeptide (PACAP): discovery and current status of research. *Regul Pept* **37**, 287–303.

Braas KM, May V, Harakall SA, Hardwick JC & Parsons RL (1998). Pituitary adenylate cyclase-activating polypeptide expression and modulation of neuronal excitability in guinea pig cardiac ganglia. *J Neurosci* **18**, 9766–9779.

Christofi FL & Wood JD (1993). Effects of PACAP on morphologically identified myenteric neurons in guinea pig small bowel. *Am J Physiol* **264**, G414–G421.

Crowcroft PJ, Holman ME & Szurszewski JH (1971). Excitatory input from the distal colon to the inferior mesenteric ganglion in the guinea-pig. *J Physiol* **219**, 443–461.

Dun EC, Huang RL, Dun SL & Dun NJ (1996). Pituitary adenylate cyclase activating polypeptide-immunoreactivity in human spinal cord and dorsal root ganglia. *Brain Res* **721**, 233–237.

Eggenberger M, Born W, Zimmermann U, Lerner EA, Fischer JA & Muff R (1999). Maxadilan interacts with receptors for pituitary adenylyl cyclase activating peptide in human SH-SY5Y and SK-N-MC neuroblastoma cells. *Neuropeptides* **33**, 107–114.

Ermilov LG & Kaliunov VN (1983). Activity of the neurons of the abdominal-aortic plexus in the guinea pig during preservation of its connections with the large intestine. *Fiziol Zh SSSR Im IM Sechenova* **69**, 372–397.

Ermilov LG, Lerner EA & Szurszewski JH (2001). PAC1 and VPAC receptors mediate colon distension-evoked slow depolarization in guinea pig inferior mesenteric ganglion neurons. *Gastroenterology* **120**, A330.

Ermilov LG, Miller SM, Schmalz PF, Hanani M, Lennon VA & Szurszewski JH (2003). Morphological characteristics and immunohistochemical detection of nicotinic acetylcholine receptors on intestinofugal afferent neurones in guinea-pig colon. *Neurogastroenterol Motil* **15**, 289–298.

Ermilov LG, Miller SM, Schmalz PF, Hanani M & Szurszewski JH (2000). The three-dimensional structure of neurons in the guinea pig inferior mesenteric and pelvic hypogastric ganglia. *Auton Neurosci* **83**, 116–126.

Ermilov LG & Szurszewski JH (1998). PACAP27 and other neuropeptides in the inferior mesenteric ganglion. *Ann N Y Acad Sci* **865**, 360–366.

Furness JB & Costa M (1987). *The Enteric Nervous System.* Churchill Livingstone, Edinburgh.

Furness JB, Kunze WA & Clerc N (1999). Nutrient tasting and signaling mechanisms in the gut. II. The intestine as a sensory organ. neural, endocrine, and immune responses. *Am J Physiol* **277**, G922–G928.

Gower WR Jr, Dietz JR, McCuen RW, Fabri PJ, Lerner EA & Schubert ML (2003). Regulation of atrial natriuretic peptide secretion by cholinergic and PACAP neurons of the gastric antrum. *Am J Physiol Gastrointest Liver Physiol* **284**, G68–G74.

Grider JR (1998). Regulation of excitatory neural input to longitudinal intestinal muscle by myenteric interneurons. *Am J Physiol* **275**, G973–G978.

Harmar AJ, Arimura A, Gozes I, Journot L, Laburthe M, Pisegna JR, Rawlings SR, Robberecht P, Said SI, Sreedharan SP, Wank SA & Waschek JA (1998). International Union of Pharmacology. XVIII. Nomenclature of receptors for vasoactive intestinal peptide and pituitary adenylate cyclase-activating polypeptide. *Pharmacol Rev* **50**, 265–270.

Jacob MH, Lindstrom JM & Berg DK (1986). Surface and intracellular distribution of a putative neuronal nicotinic acetylcholine receptor. *J Cell Biol* **103**, 205–214.

Katsoulis S, Clemens A, Schworer H, Creutzfeldt W & Schmidt WE (1993). PACAP is a stimulator of neurogenic contraction in guinea pig ileum. *Am J Physiol* **265**, G295–G302.

Kirchgessner AL & Liu MT (1998). Immunohistochemical localization of nicotinic acetylcholine receptors in the guinea pig bowel and pancreas. *J Comp Neurol* **390**, 497–514.

Kirchgessner AL & Liu MT (2001). Pituitary adenylate cyclase activating peptide (PACAP) in the enteropancreatic innervation. *Anat Rec* **262**, 91–100.

Lai CC, Wu SY, Lin HH & Dun NJ (1997). Excitatory action of pituitary adenylate cyclase activating polypeptide on rat sympathetic preganglionic neurons in vivo and in vitro. *Brain Res* **748**, 189–194.

Lomax AE, Sharkey KA, Bertrand PP, Low AM, Bornstein JC & Furness JB (1999). Correlation of morphology, electrophysiology and chemistry of neurons in the myenteric plexus of the guinea-pig distal colon. *J Auton Nerv Syst* **76**, 45–61.

Love JA & Szurszewski JH (1987). The electrophysiological effects of vasoactive intestinal polypeptide in the guinea-pig inferior mesenteric ganglion. *J Physiol* **394**, 67–84.

Ma RC & Szurszewski JH (1996). Modulation by opioid peptides of mechanosensory pathways supplying the guinea-pig inferior mesenteric ganglion. *J Physiol* **491**, 435–445.

Masuo Y, Matsumoto Y, Tokito F, Tsuda M & Fujino M (1993). Effects of vasoactive intestinal polypeptide (VIP) and pituitary adenylate cyclase activating polypeptide (PACAP) on the spontaneous release of acetylcholine from the rat hippocampus by brain microdialysis. *Brain Res* **611**, 207–215.

May V, Beaudet MM, Parsons RL, Hardwick JC, Gauthier EA, Durda JP & Braas KM (1998). Mechanisms of pituitary adenylate cyclase activating polypeptide (PACAP)-induced depolarization of sympathetic superior cervical ganglion (SCG) neurons. *Ann N Y Acad Sci* **865**, 164–175.

May V & Braas KM (1995). Pituitary adenylate cyclase-activating polypeptide (PACAP) regulation of sympathetic neuron neuropeptide Y and catecholamine expression. *J Neurochem* **65**, 978–987.

Messenger JP & Furness JB (1993). Distribution of enteric nerve cells projecting to the superior and inferior mesenteric ganglia of the guinea-pig. *Cell Tissue Res* **271**, 333–339.

Miller SM, Ermilov LG, Szurszewski JH, Hammond PI & Brimijoin S (1997). Selective disruption of neurotransmission by acetylcholinesterase antibodies in sympathetic ganglia examined with intracellular microelectrodes. *J Auton Nerv Syst* **67**, 156–167.

Miller SM & Szurszewski JH (2002). Relationship between colonic motility and cholinergic mechanosensory afferent input to mouse superior mesenteric ganglion. *Neurogastroenterol Motil* **14**, 339–348.

Miller SM & Szurszewski JH (2003). Circumferential, not longitudinal, colonic stretch increases synaptic input to mouse prevertebral ganglion neurons. *Am J Physiol Gastrointest Liver Physiol* **285**, G1129–G1138.

Mizumoto A, Fujimura M, Ohtawa M, Ueki S, Hayashi N, Itoh Z, Fujino M & Arimura A (1992). Pituitary adenylate cyclase activating polypeptide stimulates gallbladder motility in conscious dogs. *Regul Pept* **42**, 39–50.

Moro O & Lerner EA (1997). Maxadilan, the vasodilator from sand flies, is a specific pituitary adenylate cyclase activating peptide type I receptor agonist. *J Biol Chem* **272**, 966–970.

Onaga T, Harada Y & Okamoto K (1998). Pituitary adenylate cyclase-activating polypeptide (PACAP) induces duodenal phasic contractions via the vagal cholinergic nerves in sheep. *Regul Pept* **77**, 69–76.

Onaga T, Okamoto K, Harada Y, Mineo H & Kato S (1997). PACAP stimulates pancreatic exocrine secretion via the vagal cholinergic nerves in sheep. *Regul Pept* **72**, 147–153.

Parkman HP, Ma RC, Stapelfeldt WH & Szurszewski JH (1993). Direct and indirect mechanosensory pathways from the colon to the inferior mesenteric ganglion. *Am J Physiol* **265**, G499–G505.

Pisegna JR & Wank SA (1993). Molecular cloning and functional expression of the pituitary adenylate cyclase-activating polypeptide type I receptor. *Proc Natl Acad Sci U S A* **90**, 6345–6349.

Portbury AL, McConalogue K, Furness JB & Young HM (1995). Distribution of pituitary adenylyl cyclase activating peptide (PACAP) immunoreactivity in neurons of the guinea-pig digestive tract and their projections in the ileum and colon. *Cell Tissue Res* **279**, 385–392.

Rattan S & Chakder S (1997). Excitatory and inhibitory actions of pituitary adenylate cyclase-activating peptide (PACAP) in the internal anal sphincter smooth muscle: sites of actions. *J Pharmacol Exp Ther* **283**, 722–728.

Rawlings SR & Hezareh M (1996). Pituitary adenylate cyclase-activating polypeptide (PACAP) and PACAP/vasoactive intestinal polypeptide receptors: actions on the anterior pituitary gland. *Endocr Rev* **17**, 4–29.

Seebeck J, Schmidt WE, Kilbinger H, Neumann J, Zimmermann N & Herzig S (1996). PACAP induces bradycardia in guinea-pig heart by stimulation of atrial cholinergic neurones. *Naunyn Schmiedebergs Arch Pharmacol* **354**, 424–430.

Stapelfeldt WH & Szurszewski JH (1989). Neurotensin facilitates release of substance P in the guinea-pig inferior mesenteric ganglion. *J Physiol* **411**, 325–345.

Szurszewski JH, Ermilov LG & Miller SM (2002). Prevertebral ganglia and intestinofugal afferent neurons. *Gut* **51**, i6–i10.

Szurszewski JH & Miller SM (1994). Physiology of prevertebral ganglia. In *Physiology of the Gastrointestinal Tract*, ed. Johnson LR, pp. 795–877. Raven Press, New York.

Tatsuno I, Uchida D, Tanaka T, Saeki N, Hirai A, Saito Y, Moro O & Tajima M (2001). Maxadilan specifically interacts with PAC1 receptor, which is a dominant form of PACAP/VIP family receptors in cultured rat cortical neurons. *Brain Res* **889**, 138–148.

Uchida D, Tatsuno I, Tanaka T, Hirai A, Saito Y, Moro O & Tajima M (1998). Maxadilan is a specific agonist and its deleted peptide (M65) is a specific antagonist for PACAP type 1 receptor. *Ann N Y Acad Sci* **865**, 253–258.

Vaudry D, Gonzalez BJ, Basille M, Yon L, Fournier A & Vaudry H (2000). Pituitary adenylate cyclase-activating polypeptide and its receptors: from structure to functions. *Pharmacol Rev* **52**, 269–324.

Weems WA & Szurszewski JH (1978). An intracellular analysis of some intrinsic factors controlling neural output from inferior mesenteric ganglion of guinea pigs. *J Neurophysiol* **41**, 305–321.

Yahagi N, Akiyama T & Yamazaki T (1998). Effects of omega-conotoxin GVIA on cardiac sympathetic nerve function. *J Auton Nerv Syst* **68**, 43–48.

## Acknowledgements

The authors are grateful to Dr E. A. Lerner for providing maxadilan and anti-maxadilan M65 peptides, to Dr A. Arimura for providing anti-serum against PAC1-R, to Sylvia Casey and Gary Stoltz for technical assistance and to Jan Applequist for help in preparing this manuscript. This work was supported by NIH Grant DK 17632.